Design and Control of Dimethyl Carbonate–Methanol Separation via Pressure-Swing Distillation

ARTICLE *in* INDUSTRIAL & ENGINEERING CHEMISTRY RESEARCH · APRIL 2013

Impact Factor: 2.59 · DOI: 10.1021/ie3034976

8 AUTHORS, INCLUDING:

Ning Zhao
Chinese Academy of Sciences
131 PUBLICATIONS **1,897** CITATIONS
SEE PROFILE

Yuhan Sun
Chinese Academy of Sciences
601 PUBLICATIONS **7,508** CITATIONS
SEE PROFILE

I&EC research
Industrial & Engineering Chemistry Research

Article

pubs.acs.org/IECR

Design and Control of Dimethyl Carbonate−Methanol Separation via Pressure-Swing Distillation

Hong-Mei Wei,[†,‡] Feng Wang,[†] Jun-Liang Zhang,[§] Bo Liao,[⊥] Ning Zhao,*[,†] Fu-kui Xiao,[†] Wei Wei,*[,†,∥] and Yu-Han Sun*[,⊥]

[†]State Key Laboratory of Coal Conversion, Institute of Coal Chemistry, Chinese Academy of Sciences, Taiyuan 030001, P.R. China

[‡]University of the Chinese Academy of Sciences, Beijing 100049, P.R. China

[§]Chemical Engineering Process Design Centre, Institute of Coal Chemistry, Chinese Academy of Sciences, Taiyuan 030001, P.R. China

[⊥]Low Carbon Conversion Center, Shanghai Advanced Research Institute, Chinese Academy of Sciences, Shanghai 201203, P.R. China

[∥]Center for Greenhouse Gas and Environmental Engineering, Shanghai Advanced Research Institute, Chinese Academy of Sciences, Shanghai 201203, P.R. China

ABSTRACT: Separation of dimethyl carbonate/methanol azeotropic mixture by using distillation process has been a hot-point in the study of the synthesis process of dimethyl carbonate by urea methanolysis method. Most studies focus on the steady-state design, and only few papers have dealt with the dynamic performance and control of this binary azeotropic system. This paper explores the design and control of pressure-swing distillation systems for separation of dimethyl carbonate/methanol. The steady-state and dynamic simulations are carried out with Aspen Plus and Aspen Dynamics. Then, on the basis of the global economical analysis, an optimized separation configuration is proposed. The vital operating parameters and geometric parameters are determined according to the simulation and optimization results. Furthermore, two control strategies, CS1 and CS2, are proposed. With disturbance, the proposed basic control structure (CS1) can only maintains the quality specification of products from the bottom of the first column. However, the second control structure (CS2) succeeds in holding the bottom product purity for two distillation columns, even for large feed flow rate and large composition disturbances. Detailed analysis for CS1 and CS2 is made based on dynamic simulation which illustrates that the control structure CS2 outperforms CS1 to handle the disturbances.

1. INTRODUCTION

Dimethyl carbonate (DMC) is a novel "green" chemical agent which has drawn great attention.[1,2] It is employed as a "green" alternative to conventional methylating and acylating agents primarily because it is nontoxic and biodegradable.[3,4] It is also used as an oxygenated fuel additive of gasolineor diesel oil, to replace the methyl-tert-butyl ether (MTBE).[5] In addition, DMC can reduce the surface tension of diesel boiling range fuels, thereby giving better injection delivery and spray. A further significant advantage of DMC over other fuel additives is that DMC could slowly decompose to CO_2 and methanol, which have no serious environmental impact.[6]

There are several methods available for the preparation of DMC.[7−14] A newly derived route for synthesis of DMC by the urea methanolysis method is considered as a green routine for the following advantages: First of all, urea and methanol (ME) are used as raw materials, which have abundant resources and are priced low. Second, the method has other advantages such as it being a safe and simple process, having higher activity of reaction, and having higher selectivity of the product, and thus, it could significantly lower the production cost of DMC. Third, byproduct ammonia can be recycled directly to the urea work to produce urea with zero emission of the byproduct. Therefore, this process is environmentally-friendly.[15−18]

However, the products of DMC and ME form a minimum-boiling azeotrope. Further separation of this azeotropic mixture is essential to obtain pure DMC product and pure methanol.

The process study of azeotrope separation for this system has been extensively studied in the literature.[19−23] Two of the most common methods for separating the binary homogeneous azeotrope are extractive distillation[24−27] and pressure-swing distillation (PSD).[28] Extractive distillation method is energy-efficient if a suitable solvent can be found but may cause environmental problems. Pressure-swing distillation is used when the azeotropic temperature and composition are sensitive to the operating pressure. A two-column system can be used to achieve the desired separation. It may cause high energy cost, but it is an environmentally friendly process and does not require additional separating agents. So it has been widely used in DMC industrial production.[29]

Several schemes have been proposed to separate DMC/ME mixtures via pressure-swing in a large collection of literature. Li

Special Issue: Multiscale Structures and Systems in Process Engineering

Received: December 20, 2012
Revised: March 28, 2013
Accepted: March 28, 2013
Published: March 28, 2013

Table 1. Azeotropic Compositions of Experimental[42] and Calculated Data at Different Pressures

				azeotropic compositions [%, ω]					
	temperature [°C]			DMC			ME		
pressure [MPa]	exp[42]	cal	RD [%]	exp[42]	cal	RD [%]	exp[42]	cal	RD [%]
0.1013	64	63.75	−0.074	30.0	29.58	−1.400	70.0	70.42	0.600
0.2026	82	82.66	0.186	26.6	26.33	−1.002	73.4	73.67	0.368
0.4052	104	104.12	0.032	20.7	21.1	−2.319	79.3	78.82	0.605
0.6078	118	118.03	−0.008	17.5	17.52	−0.114	82.5	82.48	0.024
0.8104	129	128.59	0.102	14.8	14.53	1.824	85.2	85.47	−0.317
1.013	138	137.2	0.195	12.4	11.97	3.468	87.6	88.03	0.491
1.519	155	153.83	0.273	7.0	6.65	5.000	93.0	93.35	0.376

[a]RD means relative deviation.

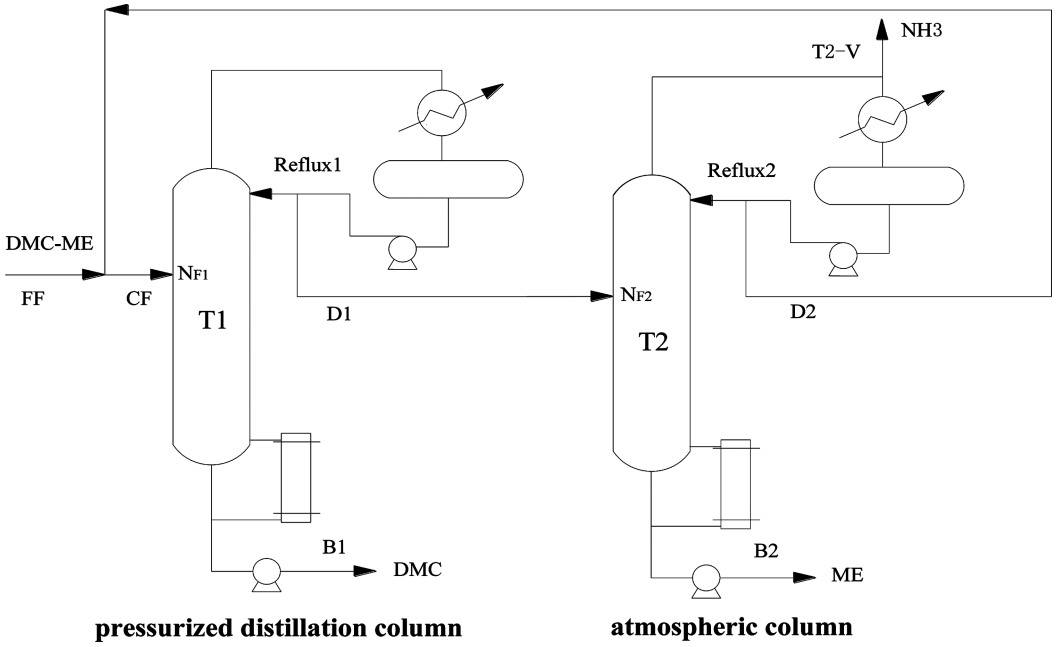

Figure 1. Conceptual design flowsheet for pressured-atmospheric system.

et al.[30] has proposed a pressured-atmospheric series separation process based on UNIQUAC equations. Wang et al.[31] has also proposed a pressured-atmospheric series separation based on NRTL equations, which is different from the separation process shown in the paper.[31] Zhang et al.[22] have investigated the process model for atmospheric-pressured rectification to separate the azeotrope (DMC/ME) produced by the urea methanolysis method. The simulation results reported in these documents and others show that high purity of DMC can be obtained via pressure-swing distillation. With an overview of the previous research, most of the studies mainly focus on the modeling and optimizing of separation process of the DMC/ME azeotrope. Few papers explore the dynamics and control structure of the separation process, Hsu et al.[32] have studied the design and control of DMC/ME azeotrope (produced by a transesterification reaction of methanol with ethylene carbonate) separation via extractive distillation. The dynamic simulation and control of PSD have been introduced and evaluated in many research works,[33−38] but there is no report about the design and control of this azeotrope separation by PSD, especially for the azeotrope produced by the urea methanolysis method where the concentration of DMC is very low.

In this paper, a pressured-atmospheric distillation process for the separation of DMC/ME is demonstrated. It is organized as follows: first, Wilson physical properties are selected for Aspen simulations and the rigorous simulation for DMC/ME separation process is investigated. Second, optimum operation parameters are obtained by minimizing the total annual cost (TAC) of the system. Finally, two suitable control strategies of this azeotropic distillation column system are introduced. Fresh feed composition and feed flow rate changes are used to test the closed-loop performance of the proposed control strategies and their dynamic performances are evaluated.

2. DMC-ME SYSTEM

The mixture DMC/ME forms a minimum azeotrope with the azeotropic temperature of 64 °C and the azeotropic compositions of 70 wt % ME and 30 wt % DMC under atmospheric pressure. Table 1 gives the azeotropic compositions of experimental[40] and calculated data at different pressures. It can be seen from Table 1 that when the pressure increases, the content of DMC in the azeotrope gradually decreases. For two different pressures (0.1 MPa and 1.5 MPa), the large shift in the azeotropic composition of the experimental data from 30.0 to 7.0 wt % indicates that a pressure-swing separation should be feasible. Aspen Plus is used

dx.doi.org/10.1021/ie3034976 | Ind. Eng. Chem. Res. 2013, 52, 11463−11478

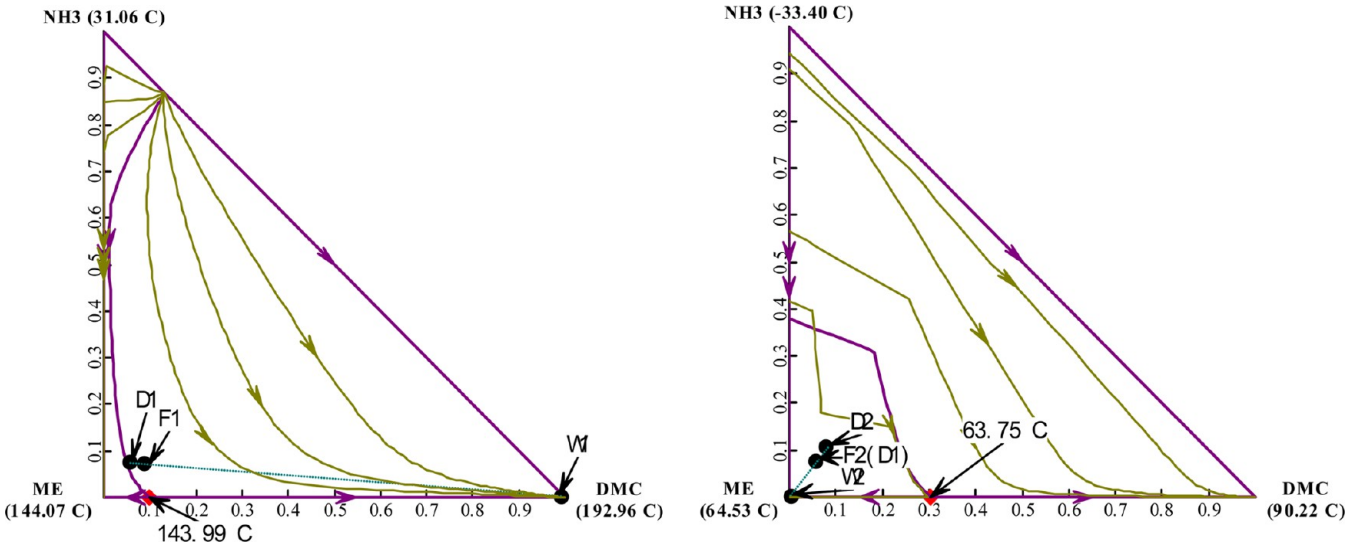

Figure 2. Residue curve map for the ternary of DMC/ME/NH_3 at (A) 1.2 and (B) 0.1 MPa.

for the steady-state simulation. The vapor phase of the system is assumed to be ideal, and the Wilson model is used to describe the nonideality of the liquid. The parameters of the Wilson model are obtained from Ma et al.[39] All other physical properties, such as vapor, enthalpies, and densities of liquid etc., are obtained from Aspen Plus databank.

The comparison of calculated values with experimental data from literature[41] at different pressures can also be seen in Table 1. It is noticed that the calculated results agree well with the experimental data in literature. On the basis of the comparison, the Wilson equation can accurately calculate all binary interaction parameters and phase equilibrium constant K for the DMC/ME system; therefore, it is reliable for the thermodynamic calculations of the DMC/ME azeotropic system.

3. DMC-ME SYSTEM STEADY-STATE DESIGN

3.1. Process Design. In the paper, the initial data used is obtained from the pilot test of 300 t/a DMC synthesis process through the urea methanolysis method. The pressured-atmosphere process is simulated with the following data: the feed is a mixture made up of 89 wt % ME, 11 wt % DMC, with a very small quantity of impurities NH_3 (0.099 wt %) . The steady-state simulation is implemented by commercial software Aspen Plus, the Wilson activity model is chosen as the property package in the simulation, and the built-in binary interaction parameters are used. The two product specifications are set as follows: the ME impurity at the bottom of the pressurized distillation column is less than 0.5 wt %, and the ME product at the bottom of atmospheric column has a purity of 99.5 wt %.

The process flow sheet for this separation system can be seen in Figure 1 with the conceptual material balance lines in Figure 2. In Figure 1, the fresh feed (FF) combines with the distillate from the atmospheric column (D2) which is the point (FF + D2) in Figure 2. It is separated into pure DMC at the bottom of the pressurized distillation column. The vapor from the top of the pressurized distillation column is close to a new azeotrope with 86 wt % ME and 14 wt % DMC. This vapor stream is split into two liquid phases after subcooling to 65 °C. The reflux1, which contains a significant amount of DMC, is designed to be return to the pressurized distillation column. The vapor from the top of atmospheric column is evacuated to remove ammonia. The stream from the bottom of the atmospheric column (B2) is ME with high purity and the distillate (D2) is recycled back to the pressurized distillation column.

Figure 2A gives the residue curve map (RCM) for the DMC/ME/NH_3 system at 1.2 MPa, Figure 2B gives the RCM for the DMC/ME/NH_3 system at 0.1 MPa. The purple curves represent distillation boundary. It is noted that both the D and B points in each RCM lie on the same side of the distillation boundary regions, and these points lie near a residue curve. Therefore, this should be a feasible design.

A distillation column still has several design degrees of freedom when the feed and pressure have been fixed, which includes the number of trays (N_T), the feed tray location (N_F), the distillate flow rate D, and the reflux ratio RR. Economic optimization is conducted to determine the number of trays (N_T), which will be discussed in detail in the next section.

3.2. Economic Optimization. Total annual cost (TAC) is adopted as the objective function to be minimized by adjusting the design parameters, including the number of trays in each zone, the feed location in the column, etc. The TAC is defined as[42]

$$\text{TAC} = \frac{\text{capitical cost}}{\text{payback year}} + \text{energy cost} \tag{1}$$

The major pieces of equipment for the DMC/ME separation process are the two column vessels and the two heat exchangers (reboiler and condenser). Other items such as pumps, valves, pipes, and the reflux drums are usually not considered because their costs are usually greatly less than the costs of the vessels and heat exchangers. Therefore, the capital cost is the sum of the heat exchanger cost (hx) and the column vessel capital cost (shell):

$$\text{capital} = \text{shell} + hx \tag{2}$$

Table 2[26,42] gives the economic parameter values and the sizing relationships and parameters used, where the A_R and A_C are the areas of the heater exchanger and the condenser, respectively, with units of squared meters; D is the inside diameter of the column, with units of meters; L is the length of the vessel, with units of meters.

dx.doi.org/10.1021/ie3034976 | Ind. Eng. Chem. Res. 2013, 52, 11463−11478

Table 2. Basis of Economics

condensers
heat-transfer coefficient = 0.852 kW/K·m^2
differential temperature = 112 °C (pressurized distillation column)/87.3 °C (atmospheric column)
capital cost = 7296$A_C^{0.65}$ where area is in squared meters
reboilers
heat- transfer coefficient = 0.568 kW/K·m^2
differential temperature = 57.7 °C (pressurized distillation column)/36.5 °C (atmospheric column)
capital cost = 7296$A_R^{0.65}$ where area is in squared meters
column vessel
capital cost = 17 640$D^{1.066}L^{0.802}$ where D and L are in meters
energy cost = \$4.7/10^6 kJ
payback period = 3 y

The size of the two columns were determined by using the "tray sizing" function in Aspen Plus and a sieve plate was selected. The heat transfer areas for the condenser and reboiler are determined based on the overall heat transfer coefficient and the differential temperature. The heat exchange areas of condenser and reboiler are calculated according to the following formula:

$$A_R = \frac{Q_R \times 1.055 \times 2.54e^6}{3600 \times 0.7457 \times \Delta T_R U_R} \quad (3)$$

$$A_C = \frac{Q_C \times 1.055 \times 2.54e^6}{36000 \times .7457 \times \Delta T_C U_C} \quad (4)$$

Where Q_R and Q_C are the reboiler duty and condenser duty with units of GJ/h; ΔT_R and ΔT_C are the differential temperatures for the reboiler and condenser with units of degrees celcius; U_R and U_C are the overall heat transfer coefficients for reboiler and condenser with units of kilowatts per degrees celcius squared meters, taken from Luyben's book.[43]

The design variables to be determined include the total stages (N_{T1}) and fresh feed tray location (N_{F1}) of the pressurized distillation column and total stages (N_{T2}) and fresh tray location (N_{F2}) of the atmospheric column. The two design specifications for all the Aspen simulations are to set 99.5 wt % of DMC at the bottom of the pressurized distillation column and 99.5 wt % of ME at the bottom of the atmospheric column. The above two design specifications are satisfied by manipulating the reflux ratio (RR) and the distillate rate (D). So many design variables need to be optimized, it is important to simplify the optimization procedure. Therefore, a calculation sequence is carefully established to facilitate the optimization. The sequential iterative optimization procedure is used to find the optimal design with the total stages N_T as the outer iterative loop and N_F as the inner iterative loop. The optimization procedure to minimize the TAC is summarized below.

1 Optimization for pressurized distillation column (T_1):
   (1) Fix two column pressure (P_1, P_2) at 1.2 MPa and 0.1 MPa.
   (2) Guess the total stages of atmospheric column (N_{T2}).
   (3) Guess the total stages of pressurized distillation column (N_{T1}).
   (4) Guess the fresh feeding location (N_{F1}).
   (5) Use the "Design/Spec/Vary" function to adjust the reflux ratio (RR_1) and distillate rate (D_1) until the two design specifications can be met.
   (6) Go back to step 4 and change N_{F1} until $Q_{R1} + Q_{R2}$ is minimized.

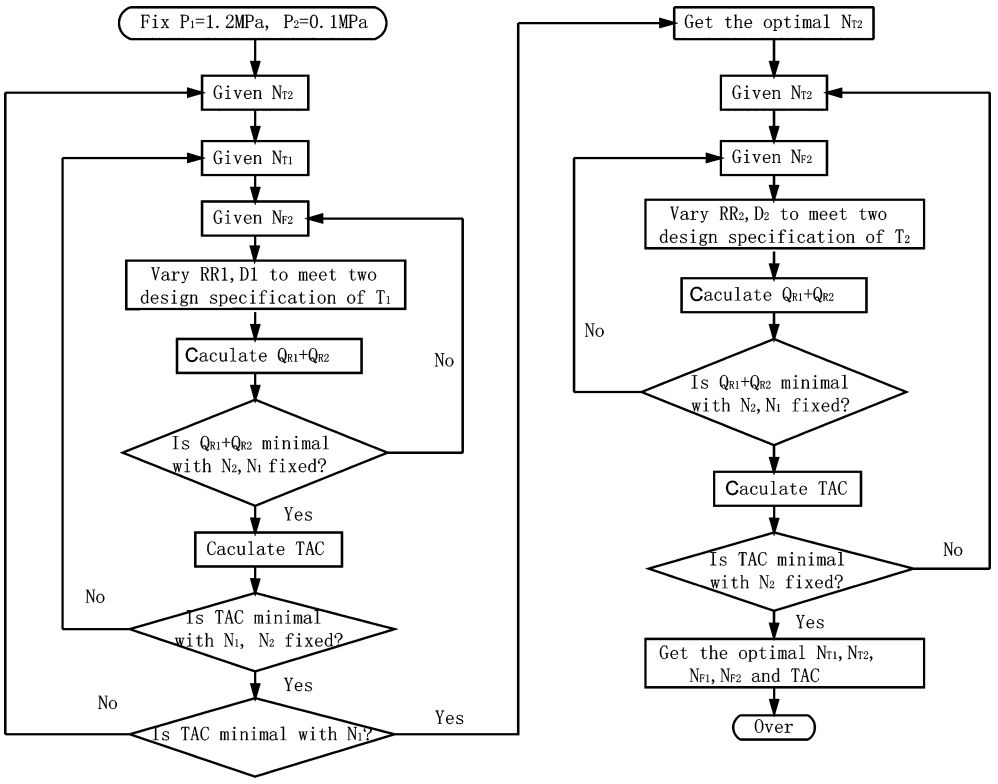

Figure 3. Sequential iterative optimization produce.

dx.doi.org/10.1021/ie3034976 | Ind. Eng. Chem. Res. 2013, 52, 11463−11478

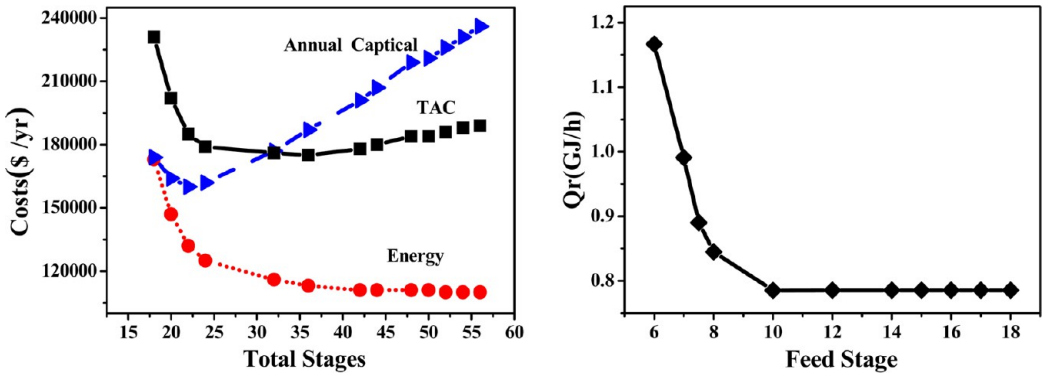

Figure 4. (A) TAC vs stages for the pressurized distillation column. (B) Q_R vs feed location for the pressurized distillation column.

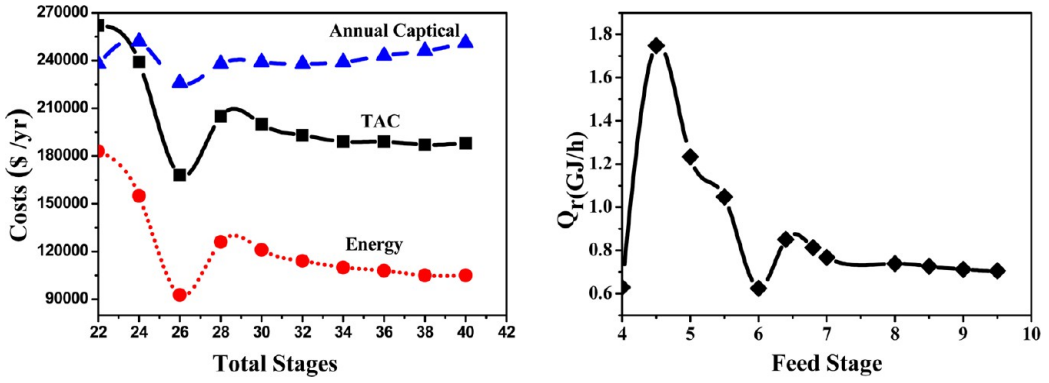

Figure 5. (A) TAC vs stages for the atmospheric column. (B) Q_R vs feed location for the atmospheric column.

(7) Go back to step 3 and change N_{T1} until TAC is minimized.

2. Optimization for atmospheric column (T_2):
   (1) Fix total stages of pressurized distillation column (N_{T1}) that has been optimized.
   (2) Guess the total stages of atmospheric column (N_{T2}).
   (3) Guess the feeding location of T_2 (N_{F2}).
   (4) Use the "Design/Spec/Vary" function to adjust the reflux ratio (RR_2) and distillate column (D_2) until the two specifications can be met.
   (5) Go back to step 3 and change N_{F2} until $Q_{R1} + Q_{R2}$ is minimized.
   (6) Go back to step 2 and change N_{T2} until the TAC is minimized.

Such a sequential iterative optimization procedure is clearly demonstrated in Figure 3.

Figures 4 and 5 give the change of the total TAC of two columns along with N_T. It is observed that the optimum total stage number N_{T1} of the pressurized distillation column is 32 with feed location N_{F1} at the 10th stage, and the optimum total stage number N_{T2} of the atmospheric column is 26 with the feed location N_{F2} at the seventh stage. The total stage number is counted from the top to the bottom with the condenser/reflux drum as the first stage and the reboiler as the last stage. The condenser is assumed to be a total condenser with liquid temperature at its boiling point. The optimal design variables and the minimum TAC of this pressure-swing system are shown in Table 3.

Figure 6 gives the final optimal flowsheet for this system, with detailed stream information, heat duties, equipment sizes, and operating conditions for steady-state mode. Figure 7 shows

Table 3. Design Variables and TAC of Pressure-Swing Columns

pressurized distillation column	N_{stage}	32
	feed stage	10
	D (m)	0.53
	Q_R (GJ/h)	0.7852
	Q_C (GJ/h)	0.7011
	A_C (m^2)	7.3288
	A_R (m^2)	15.8025
	shell ($10^6)	0.107
	HX ($10^6)	0.0705
	energy ($10^6/y)	0.116
	capital ($10^6)	0.177
	TAC ($10^6/y)	0.176
atmospheric column	N_{stage}	26
	feed stage	7
	D (m)	0.63
	Q_R (GJ/h)	0.62
	Q_C (GJ/h)	1.01
	A_C (m^2)	32.2683
	A_R (m^2)	19.0183
	shell ($10^6)	0.10715
	HX ($10^6)	0.11928
	energy ($10^6/y)	0.092551
	capital ($10^6)	0.226430
	TAC ($10^6/y)	0.16803

the temperature profiles of the two columns for the flowsheet in Figure 6. As you can see from Figure 7A and C, there is a fairly substantial rise in the temperature on stage 29 for high pressurize coumn and a rapid rise on stage 6 for the atmospheric column. These indicate the proper temperature

dx.doi.org/10.1021/ie3034976 | Ind. Eng. Chem. Res. 2013, 52, 11463−11478

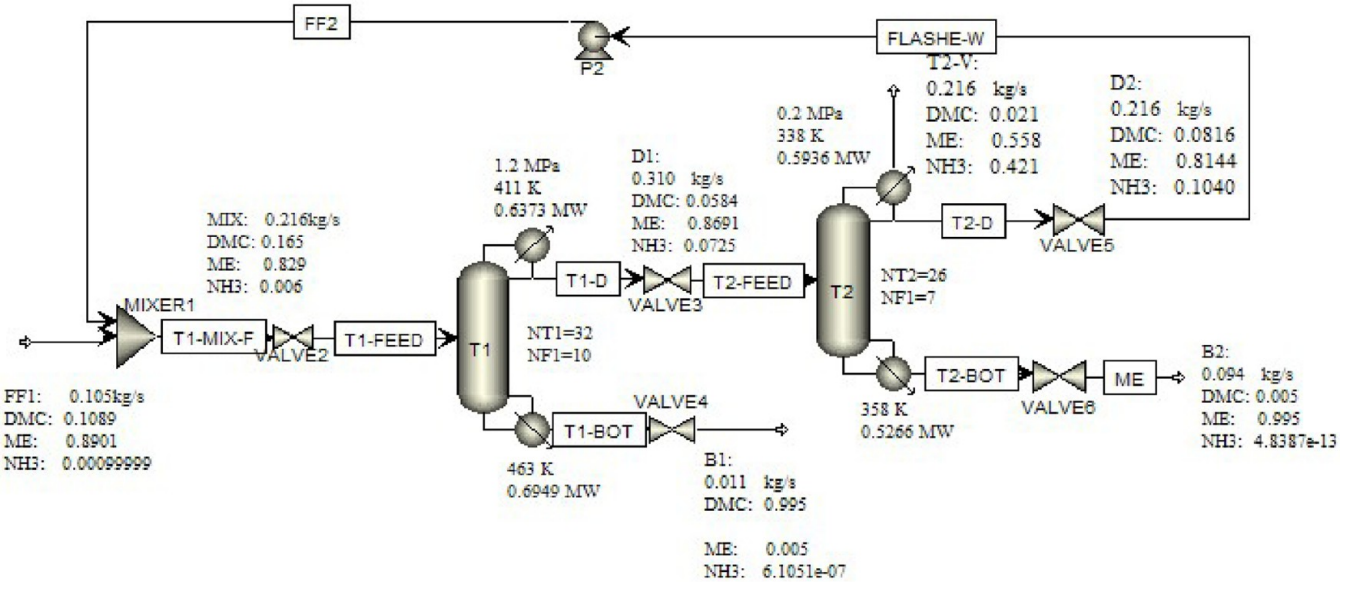

Figure 6. Flowsheet for the pressure-swing distillation system: DMC/ME system.

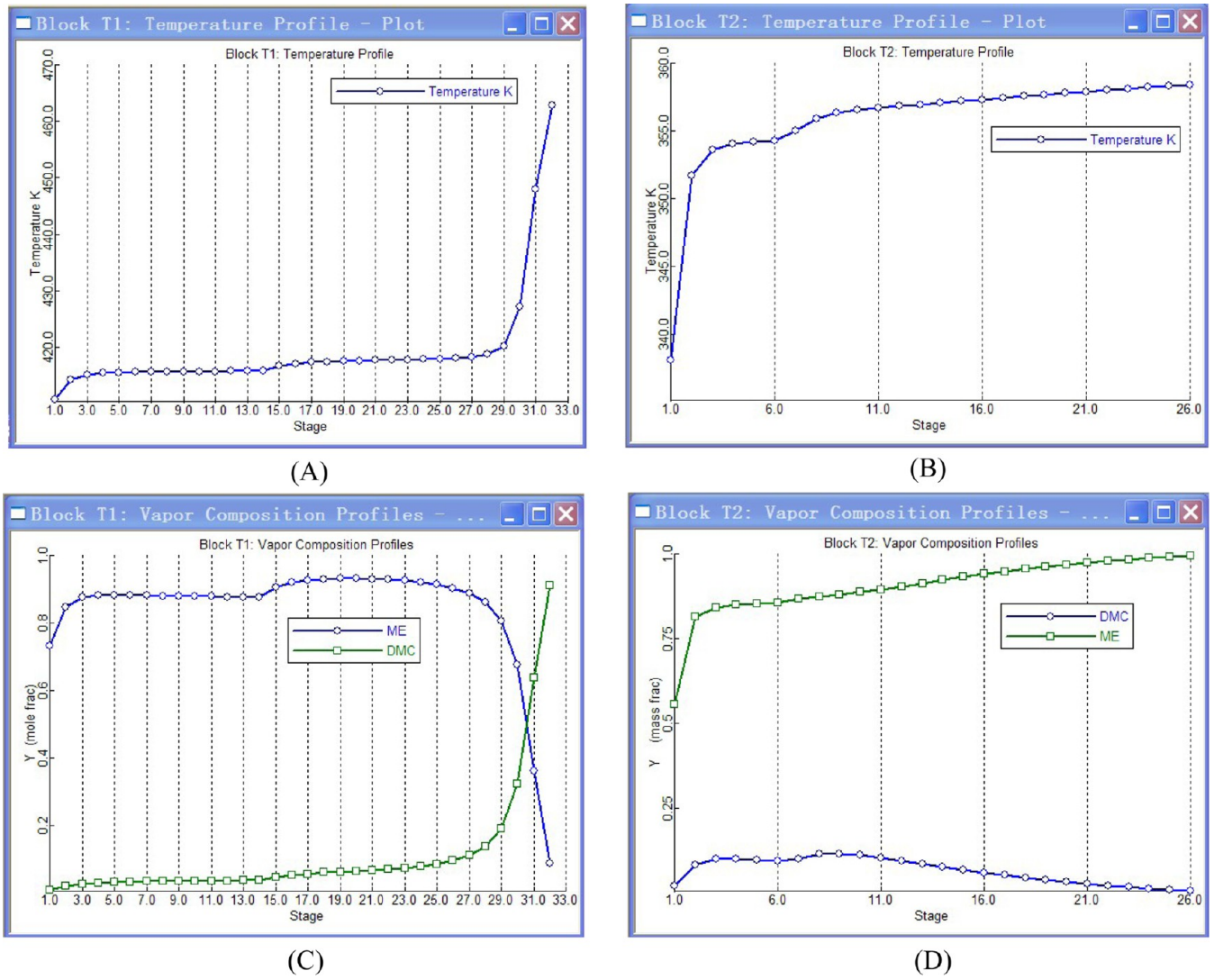

Figure 7. (A) Temperature profile in pressurized distillation column; (B) composition profiles in pressurized distillation column; (C) temperature profile in atmospheric column; (D) composition profiles in atmospheric column.

dx.doi.org/10.1021/ie3034976 | *Ind. Eng. Chem. Res.* 2013, 52, 11463−11478

control points for the two columns. At these points, it is noticed from Figure 7B and D that the DMC purity for the pressurized distillation column raises rapidly to 99.5 wt %, while the ME purity slips down rapidly to zero. Simultaneously, the ME purity in the atmospheric column raises gradually from 55.6 to 99.5 wt % and the DMC purity decreases gradually from 2.09 to 0.7 wt %.

4. CONTROL STRATEGY FOR THE OVERALL PROCESS

In this section, two control strategies for the pressurized-atmospheric distillation process are developed with the parameters determined by minimization of TAC. First, it is necessary to define the equipment size of the two distillation columns before a steady-state simulation is converted to a dynamic one. Therefore, the tray-sizing option in Aspen Plus is utilized to calculate the column size of the two columns. The calculation results are shown in Table 4.

Table 4. Size of the Reflux Drum and the Sump

	pressurized distillation column	atmospheric Column
column diameter (m)	0.534	0.630
side weir length (m)	0.390	0.384
volume flow (m^3/s)	0.00131182	0.00101776
reflux drum diameter (m)	0.8	1.6
reflux drum length (m)	0.2	0.4
sump diameter (m)	0.8	1.6
sump length (m)	0.4	0.8

The Aspen Plus file is exported to Aspen Dynamics as a pressure-driven simulation after reflux drum and base volumes are specified to provide 5 min of holdup when the vessels are 50% full. Pumps and valves are inserted to provide adequate pressure drops over valves for good rangeability. Most valves are specified to have pressure drops of 3 atm. The default control scheme is modified as discussed in the following section.

4.1. Basic Control Structure CS1. The basic control structure evaluated for this two-column system is shown in Figure 8. Conventional PI (proportional and integral) controllers are used for all flows, pressures, and temperatures. The features of the loops are outlined as below:

1. The feed is flow-controlled.
2. The pressure in each column is controlled by manipulating condenser heat removal.
3. The reflux drum level in each column is controlled by manipulating distillate.
4. The base level of each column is controlled by manipulating the bottom flow rate.
5. The tray temperature in each column is controlled by manipulating the reboiler heat input in that column.
6. Reflux flow rate in each column is controlled by R/F ratio. In the pressurized distillation column, the ratio is denoted by R_1/F_1. In the atmospheric column, the ratio is denoted by R_2/F_2.

An important feature of control loop in the pressure-swing system is to maintain the product purity by manipulate the critical tray temperature. Since both product streams are at the bottom of two columns, the trays selected for temperature control are located near the bottom of each column where the temperatures change rapidly. In order to obtain DMC product with high purity in the pressurized column, temperature at stage 29 will be held at 147.10 °C, and the set point of temperature at stage 23 in the atmospheric column is chosen as 84.9 °C to maintain ME purity.

Another noteworthy feature of the CS1 is that the R/F structure is implemented by using a multiplier block for each column. Where the input of the block is the mass flow rate of the feed and the output of the multiplier block is the mass flow rate of the reflux. This R/F ratio scheme was recommended by Luyben[43] and Grassi[44] to maintain product purities in the face of feed composition disturbances and feed flow rate changes.

Conventional PI controllers are used for all controllers except the four liquid level controllers. All the level controllers are proportional only with a gain of 2. Proportional and integral settings of the top pressure control loops for both columns are set at K_c = 20 and τ_1 = 12 min. Proportional and integral settings of the flow control loops for both columns are set at K_c = 0.5 and τ_1 = 0.3 min. The deadtime of temperature controller is set at 1 min. The tuning constants are determined via relay feedback test with Tyreus and Luyben tuning rules[45] provided in Aspen Dynamic. The iterative tuning procedure is to tune the temperature loop in the pressurized column first, then the atmospheric column. The procedure is repeated until the tuning parameters from relay feedback test converges. Table 5

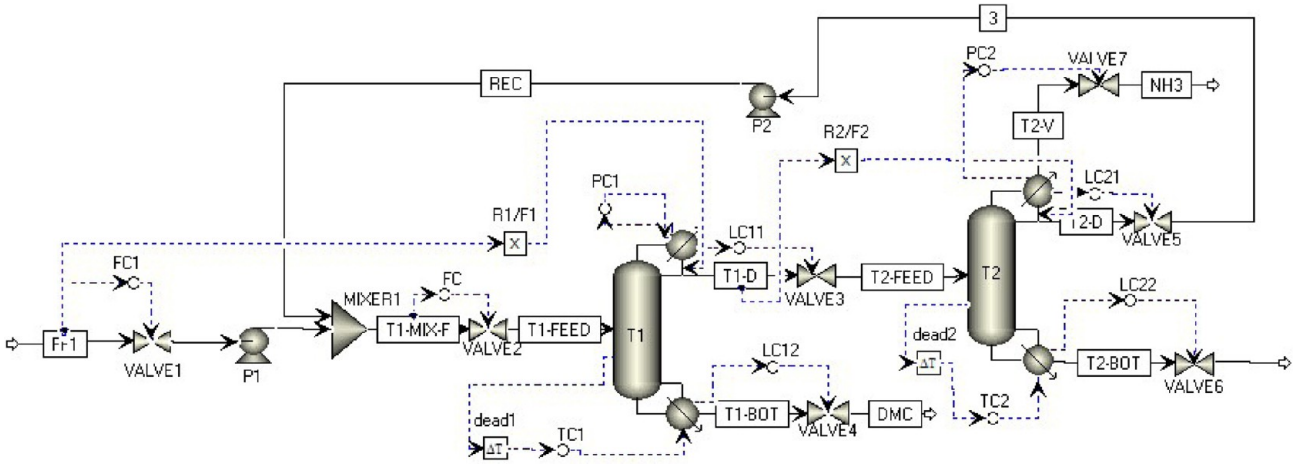

Figure 8. Control structure CS1.

dx.doi.org/10.1021/ie3034976 | Ind. Eng. Chem. Res. 2013, 52, 11463−11478

gives the tuning parameters for the two temperature controllers.

Table 5. Controller Tuning Parameters for Control Structure CS_1 and CS_2

	CS1	CS2
high-pressure column		
controlled variable (°C)		$T_{1,5}$ = 144.05
manipulatiated variable		R_1/F_1
transmitter range (°C)		100−200
controlled output range (W)		0−0.29 × 10^6
K_c		7.09
τ_1 (min)		6.6
controlled variable (°C)	T_{29} = 147.1	$T_{1,29}$ = 145.9
manipulatiated variable	Q_{R1}	Q_{R1}
transmitter range (°C)	100−200	50−200
controlled output range (W)	0−1.57 × 10^6	0−22.44 × 10^6
K_c	0.5	1.66
τ_1	3	46.2
atmospheric column		
controlled variable (°C)		$T_{2,6}$ = 82.57
manipulatiated variable		Q_{R2}
transmitter range		50−200
controlled output range (W)		0−0.72 × 10^6
K_c		2.05
τ_1		20.5
controlled variable (°C)	T_{23} = 84.9	$T_{2,23}$ = 84.9
manipulatiated variable	Q_{R2}	Q_{R2}/F_2
transmitter range (°C)	100−200	100−200
controlled output range (W)	0−1.25 × 10^6	0−1.25 × 10^6
K_c	0.5	2.14
τ_1	3	10

Feed flow rate and composition disturbances are introduced into the system to evaluate the dynamic performance. The performance of the control structure CS1 is demonstrated in Figures 9 and 10.

The responses of the system to 10% increase and decrease in feed flow rate are shown in Figure 9. The solid lines are for a step increase at 0.2 h from 0.003044 to 0.00335 kmol/h, the dashed lines for a step decrease at 0.2 h from 0.003044 to 0.00274 kmol/h. It is noticed that although a stable regulatory control is achieved for several large disturbances, it has taken almost 10 h for the product concentration at the bottom of the two columns to reach the new steady state. There is a fairly large transient drop in DMC product purity X_{B1}(DMC) down to 98.2 wt % when feed flow rate increases, but the steady-state purity recovers to 99.5 wt %. There is a relatively small transient drop in DMC product purity X_{B2}(ME) down to 99.3 wt % when feed flow rate increases, and the steady-state purity stays near 99.3 wt %, which displays slightly larger deviations from their specifications. It is also shown that the two controlled temperatures smoothly return back to their set point values.

Similar results are obtained for 20% step change in feed composition disturbances at 0.2 h. As it is shown in Figure 10, the solid lines are for a step change in feed composition from 0.042 to 0.05 (mol %) DMC, the dashed lines are for a step change from 0.042 to 0.034 (mol %) DMC.

Increase of DMC or decrease of ME in the feed leads to the increase in the bottom stream B1 and the decrease in bottom stream B2. There is a fairly small transient rise in DMC product purity X_{B1}(DMC) up to 99.51 wt % when there is more DMC in the feed, and the steady-state purity recovers to 99.5 wt %. There is a relatively small transient drop in DMC product purity X_{B2}(ME) down to 99.57 wt % from 99.59 wt % when there is more DMC in the feed, and the steady-state purity stays near 99.57 wt %, which displays slightly smaller deviations from their specifications. The two temperatures in the atmospheric column are held quite close to their set point values after a smooth transition period.

It is clear that this control structure handled feed composition changes relatively well. However, the response of the system for a feed flow rate disturbance is a little poor.

4.2. Analysis for CS1 Control. To understand the dynamic response of the CS1, the distillation principle is introduced here.

$$F + L_R = L_S \quad V_S = V_R \tag{5}$$

$$D = V_R - L_R \tag{6}$$

$$\mathrm{RR} = \frac{L_R}{D} \tag{7}$$

Formula 5 gives the mass conservation on the feed plate in distillation column, and formula 6 gives the mass conservation in the condenser in a distillation column.

The increased flows to the pressurized column eventually produce an immediately decrease in the concentration of light component at the bottom according to the distillation principle, that is, the X_{B1}(DMC) decreases immediately as the feed flow rate increase. At the same time, when the feed is increased, the application of control scheme with R/F ratio in CS1 immediately increase the reflux flow (L_R) in pressurized column. The vapor flow rate (V_R) controlled by the heat duties of the reboiler maintain unchanged in a short time for the controller with big delay, and so to the distillate (D) decreases according to formula 6. Therefore the reflux ratio of the pressurized column increase, this make more volatile components ME distillate from the top of the pressurized column and enhances the DMC concentration X_{B1}(DMC). In addition, an increase in the feed flow rate causes a temperature drop in the bottom stripping section, which causes the controller to increase the reboiler input, and then a gradually increase the reflux ratio. Therefore, the results of the interaction among these factors is that the composition of DMC sharply reduces when a +10% step change in the feed flow rate takes place at t = 0.2 h, and then gradually returns back to their set point value, as can be seen in Figure 9.

Since the distillate from the pressurized column is the feed for the atmospheric column, the reflux ratio of the atmospheric column decreases according to the same duduction discussed above. This results in more volatile components (DMC/ME azeotrope) escaping from the bottom of the atmospheric column, that is the reason why X_{B2}(ME) deviates from the set point.

Then, a control scheme with Q_R/F ratio should be added to improve the dynamic performance of CS1 for feed flow rate disturbance, which is recommended by Luyben[44] and illustrated in Yu's paper[46] in detail. The conventional control wisdom suggests that the feed forward control system with a Q_R/F and L_R/F controller could handle feed flow rate changes fairly well.

As can been seen in Figure 10, feeding more DMC and less ME produces a decrease in X_{D1}(ME) and increase in X_{B2}(DMC) at t = 0.2 h, as expected, and so increases

dx.doi.org/10.1021/ie3034976 | Ind. Eng. Chem. Res. 2013, 52, 11463−11478

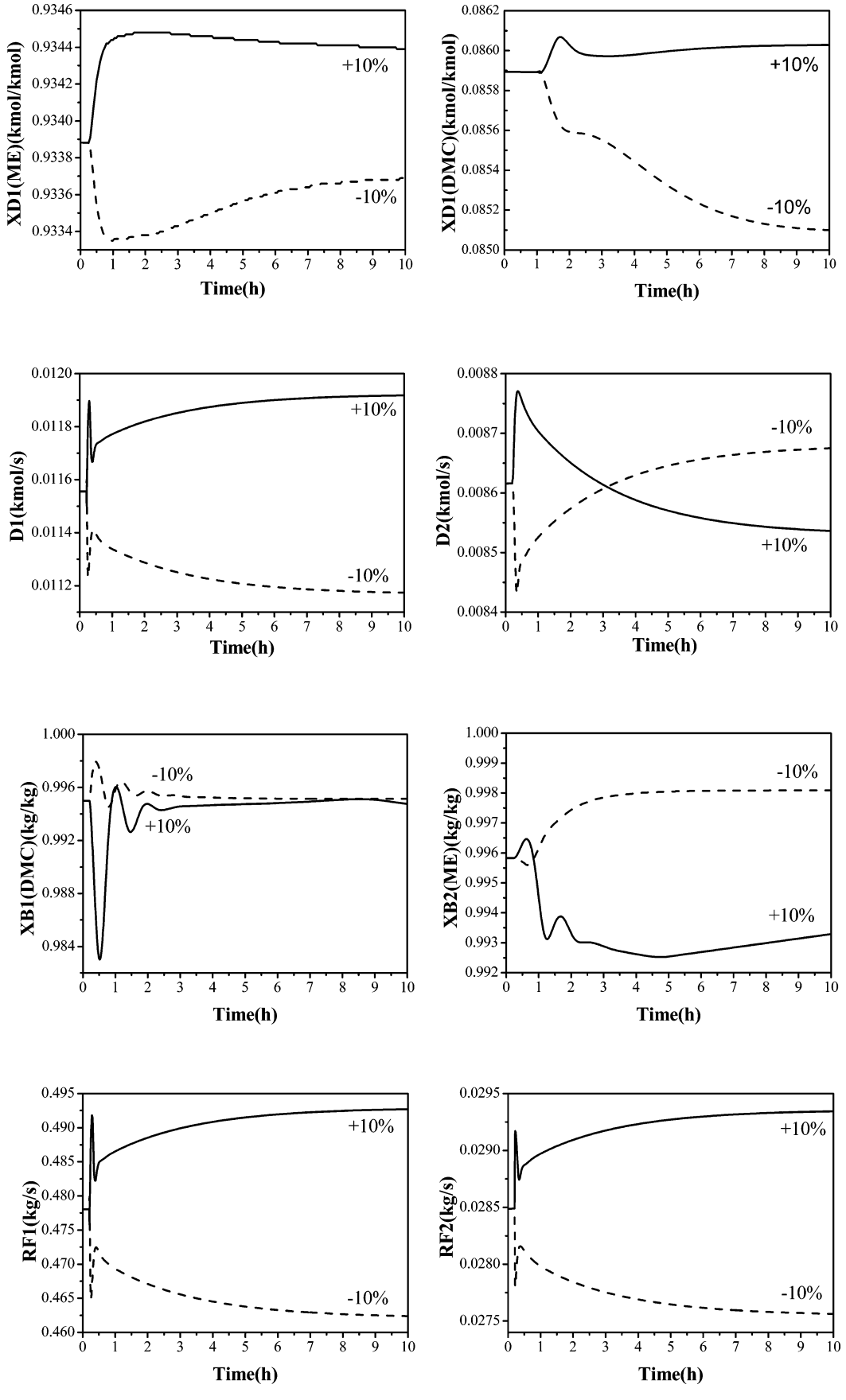

Figure 9. continued

dx.doi.org/10.1021/ie3034976 | *Ind. Eng. Chem. Res.* 2013, 52, 11463−11478

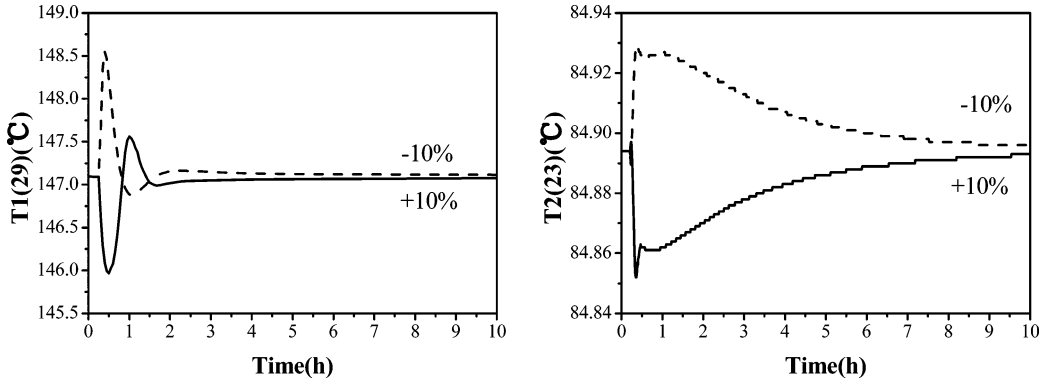

Figure 9. ±10% changes in feed flow rate.

X_{D2}(DMC) and X_{B2}(ME) at t = 0.2 h. The purity of the X_{B1}(DMC) product bottom stream from the pressurized column returns to its set point after small transient, the purity of X_{B2}(ME) product bottom stream from the atmospheric column deviates a little from its set point, this occurs because the azeotrope (DMC/ME) drops out of the bottom of the azeotropic column.

For feed composition disturbances, the deviation in product purity could be solved by using a cascade composition/temperature control (CC/TC) structure. Another solution would be to adjust the DMC/ME feed ratio to accommodate these deviations. If accurate control on product purity is required, a dual-temperature control structure can be used, which has been briefly described in Luyben's book[42] and illustrated in detail in Luyben's papers.[47] In this paper, the dual-temperature control structure is adopted.

From that mentioned above, a control structure CS2 with the Q_R/F ratio, L_R/F ratio, and a dual-temperature controller is proposed in the second control structure to further improve the performance of CS1.

The next issue is to decide the location of dual-temperature controllers. The invariant temperature criterion illustrated in Figure 11 is used, which is proposed in Luyben's work[45] and has been implemented in Luyben's paper.[47] The temperature profiles in both columns are plotted for feed compositions of 34, 42, and 50 mol % DMC when the products are all held at their specified values. The suitable locations for controllers are the trays where temperature does not change much as the feed composition changes. As shown in Figure 11, stage 5, 18 in the pressurized column and stage 5, 22 in atmospheric column satisfy this criterion. Combining the slope criterion which is displayed in Figure 7, stage 5, 29 in the pressurized column and stage 6, 23 in the atmospheric column were chosen as the temperature control points.

4.3. Improved Control Structure CS2. Figure 12 shows the developed CS2 control structure. It only differs from the CS1 structure in the following aspects:

1. The temperature on stage 6 in the atmospheric column is controlled by manipulating the reflux-to-feed ratio (R_2/F_2 ratio).
2. The temperature on stage 29 in the pressurized distillation column is controlled by manipulating the reboiler heat input-to-feed ratio (Q_{R1}/F_1).
3. The temperature on stage 23 in the atmospheric column is controlled by manipulating the reboiler heat input-to-feed ratio (Q_{R1}/F_2).

It should be noticed that the "TC1,29" and "TC2,23" controllers are on "cascade" with its set point coming from the multipliers "Q_{R1}/F_1" and "Q_{R2}/F_2". The output signal from the "$T_{1,29}$" controller is the ratio of reboiler heat input in the pressurized distillation column to the feed "Q_{R1}/F_1". The output signal from the "$T_{2,6}$" controller is the "R_2/F_2" value. The output signal from the "T_{23}" controller is the ratio of reboiler heat input in the atmospheric column to the feed Q_{R1}/F_2.

4.3.1. Analysis for the Control Structure CS2. The effectiveness of the control structure CS2 can be seen from Figures 13 and 14. It is obvious that the control strategy CS2 is more reliable than that of CS1 since the DMC purities in the two distillation columns are closed to the setting values. It could also be noticed that the system comes to a new steady state in about 5 h. Figure 13 shows how product purities vary in the face of the same scenario of feed flow rate disturbances used previously. The solid lines are for 10% feed increase, and the dashed lines are for 10% feed decrease. Increasing feed results in increases in D1 and decreases in D2 as expected. The temperature in the pressurized column is held at their set point values after a short transient period, as is the two temperatures in the atmospheric column. The purities of the two products are held quite close to their desired values. The largest offset in the DMC product purity occurs for 10% increase in feed flow rate where it drops to 98.3 wt %, but the steady-state purity recovers 99.5 wt % in about 3 h.

Figure 14 gives the responses of the system for step changes in feed composition at 0.2 h. The solid lines are for 20% DMC increase in the feed with corresponding reduction in ME, and the dashed lines are for 20% DMC decrease. Feeding more DMC and less ME produces an increase in D1 and increase in D2 as expected. There is a fairly small transient drop in DMC product purity X_{B1}(DMC) down to 99.46 wt % when more DMC is fed, but the steady-state purity recovers 99.5 wt % in about 2 h. There is also a fairly large transient drop in DMC product purity X_{B2}(ME) up to 99.7 wt % when less ME is fed, but the steady-state purity recovers 99.59 wt % in about 3 h.

For control structure CS2, which has been implemented in Repke's paper,[33] increasing feed results in increase in L_R and increase in V_S proportionately because of the application of two multiplier blocks R/F and Q_R/F, which makes the ratio of V/F constant while keeping the ratio of D/F essentially unchanged, helping to maintain the composition of the two product streams. As can be seen in Figure 13 and 14, the two bottom product purities are both held quite close to their desired values after a short transient deviation; especially, the pressurized

dx.doi.org/10.1021/ie3034976 | Ind. Eng. Chem. Res. 2013, 52, 11463−11478

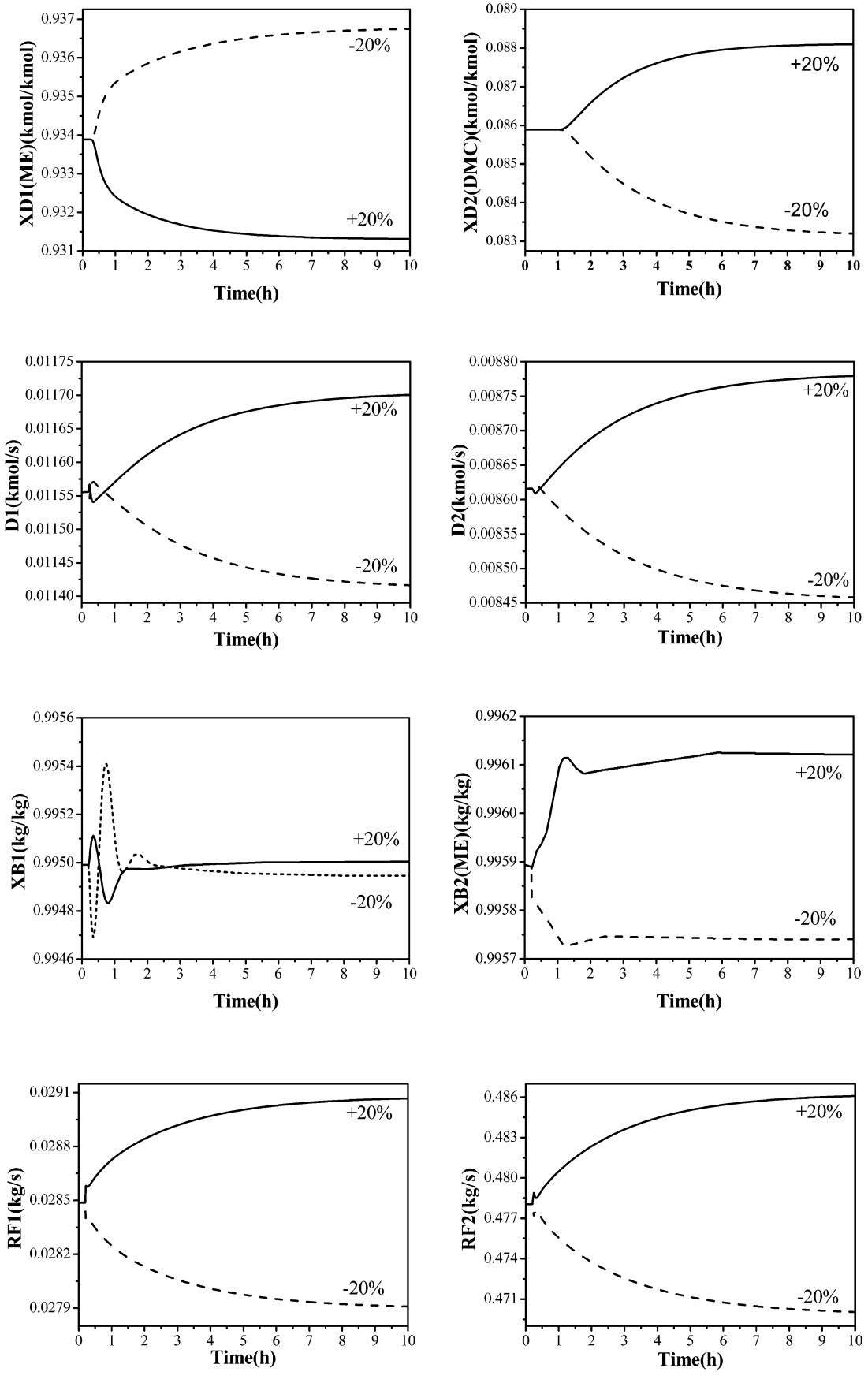

Figure 10. continued

dx.doi.org/10.1021/ie3034976 | *Ind. Eng. Chem. Res.* 2013, 52, 11463−11478

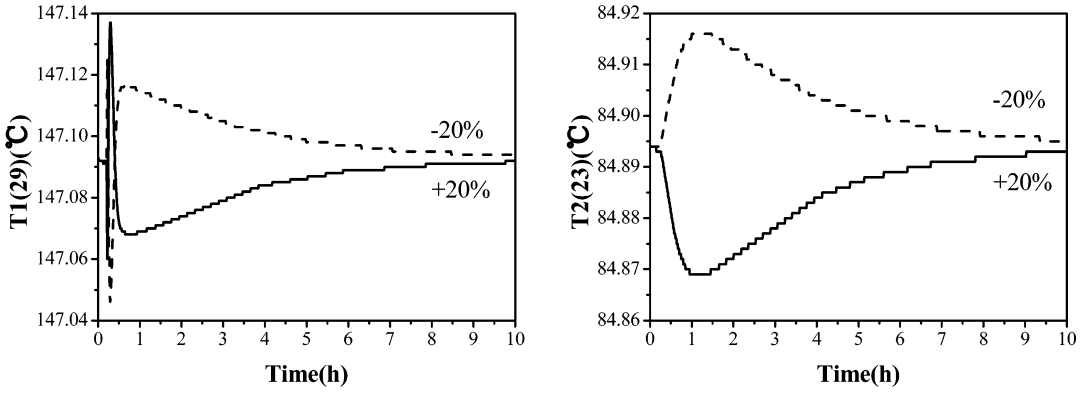

Figure 10. ±20% changes in feed composition.

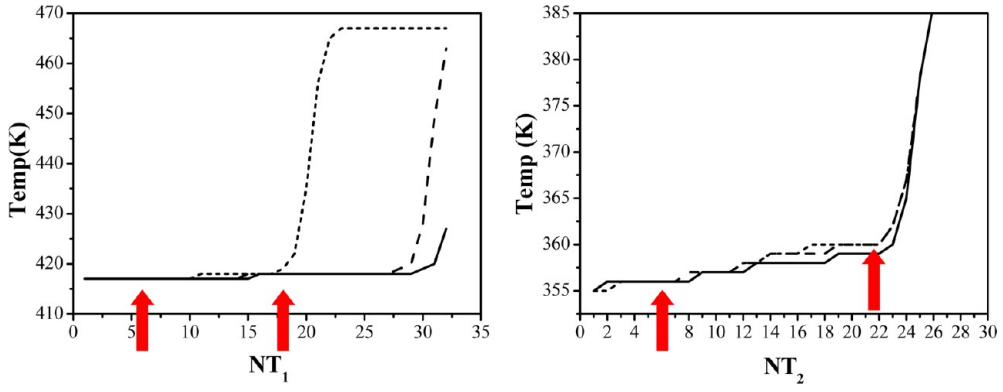

Figure 11. Temperature profiles for feed composition changes.

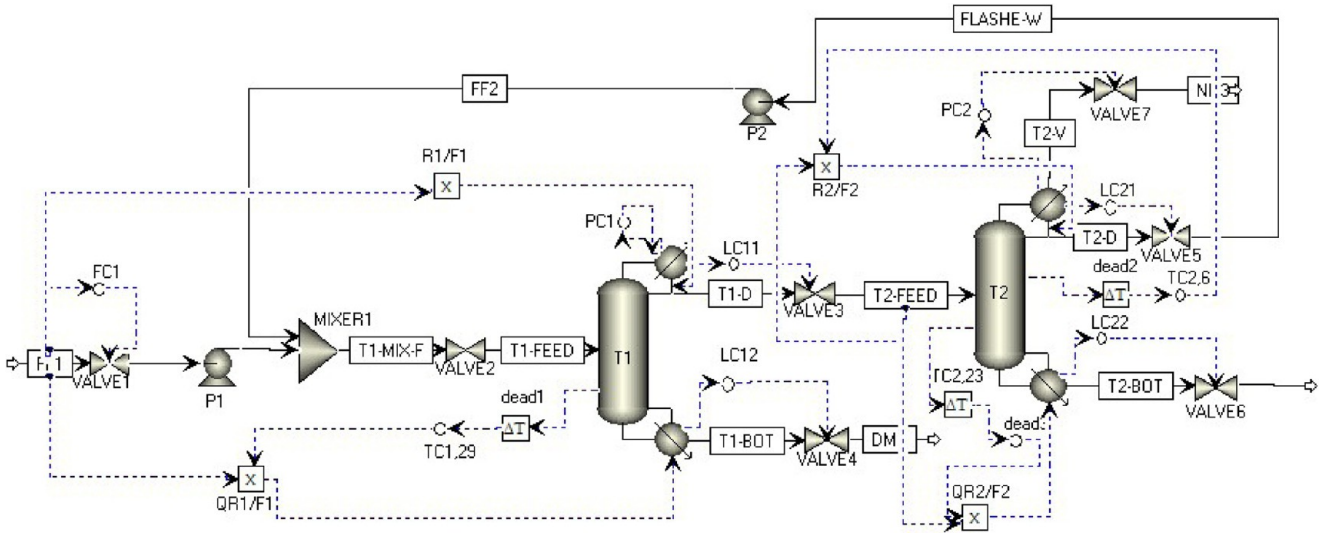

Figure 12. Control structure CS2.

column sees a gradual change in the composition X_{D1}(ME), but the composition returns to 86.0 wt % in about 5 h. There is a small offset in the purity of the DMC stream from the top of the second column.

It is worth noting that the control structure CS2 gives tighter control with smaller peak transient disturbances and a shorter settling time because of the use of dual-temperature controllers in the atmospheric column. It is also noticed that, for both feed flow rate and feed composition disturbance, the temperature in the pressurized column is held at their set point values after a short transient period, as are the two temperatures in the atmospheric column.

Consequently, the control structure CS2 would more rapidly adjust operational parameters to keep the product purity better than CS1 in the face of feed and composition disturbances.

5. CONCLUSION

The design and control of a pressure-swing distillation process for separation of a DMC/ME azeotrope has been studied in this paper. A pressured-atmospheric distillation system is

dx.doi.org/10.1021/ie3034976 | Ind. Eng. Chem. Res. 2013, 52, 11463−11478

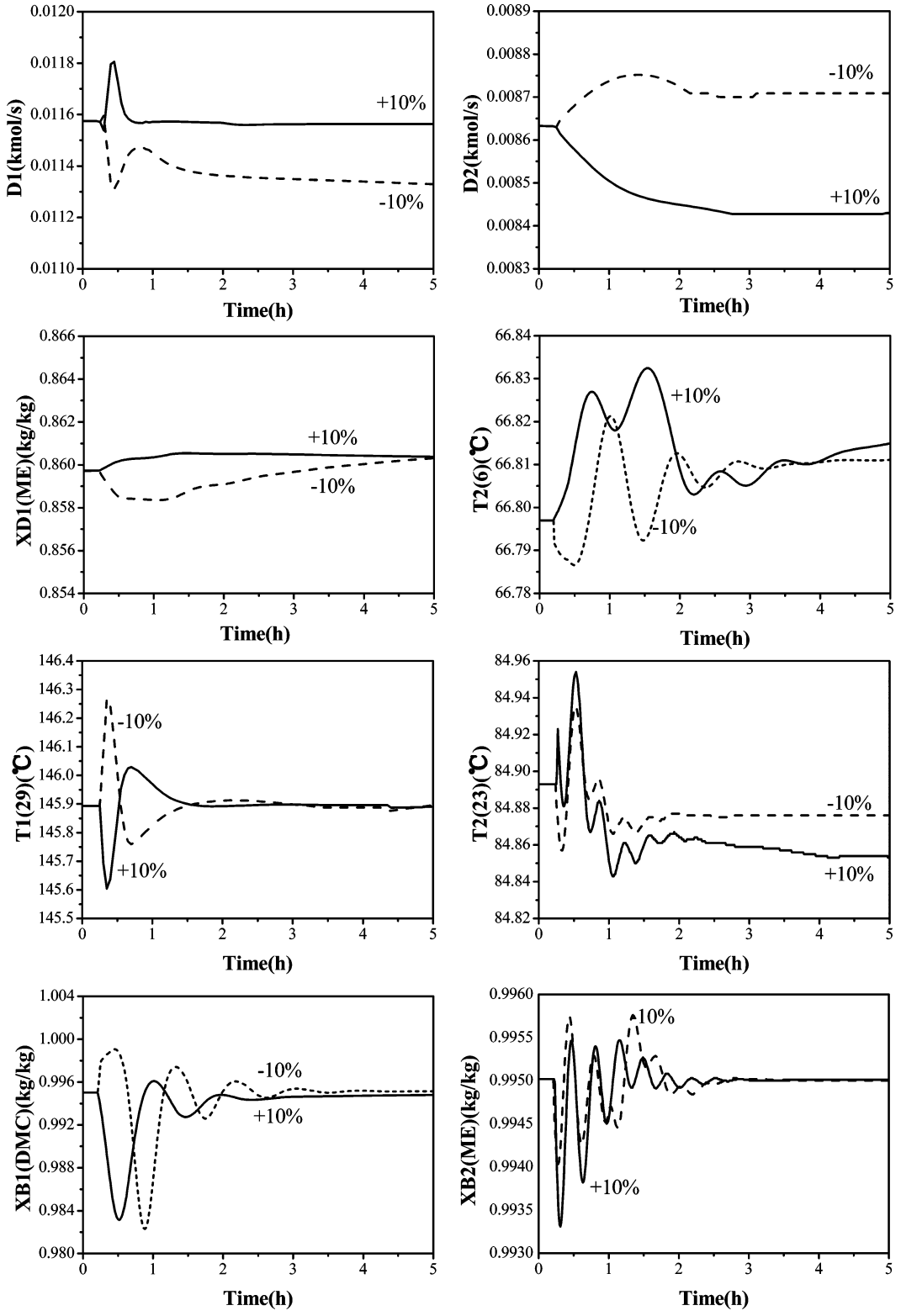

Figure 13. ±10% changes in feed flow rate.

proposed and optimized by minimizing TAC. The key operating parameters and column configurations for this system are also explored according to the steady-state simulation results.

Two plantwide control strategies are proposed and examined with this azeotropic distillation system under the feed composition and flow rate disturbances. The results show that the developed control structure CS2 outperforms the conventional control structure CS1 in keeping the product purity X_{B2}(ME) at the designed value. CS2 is proven to be considerably effective to handle the large disturbances in feed flow and feed composition, where the DMC product at the bottom of the pressurized column and ME product at the atmospheric column are both kept at their desired values.

dx.doi.org/10.1021/ie3034976 | *Ind. Eng. Chem. Res.* 2013, 52, 11463−11478

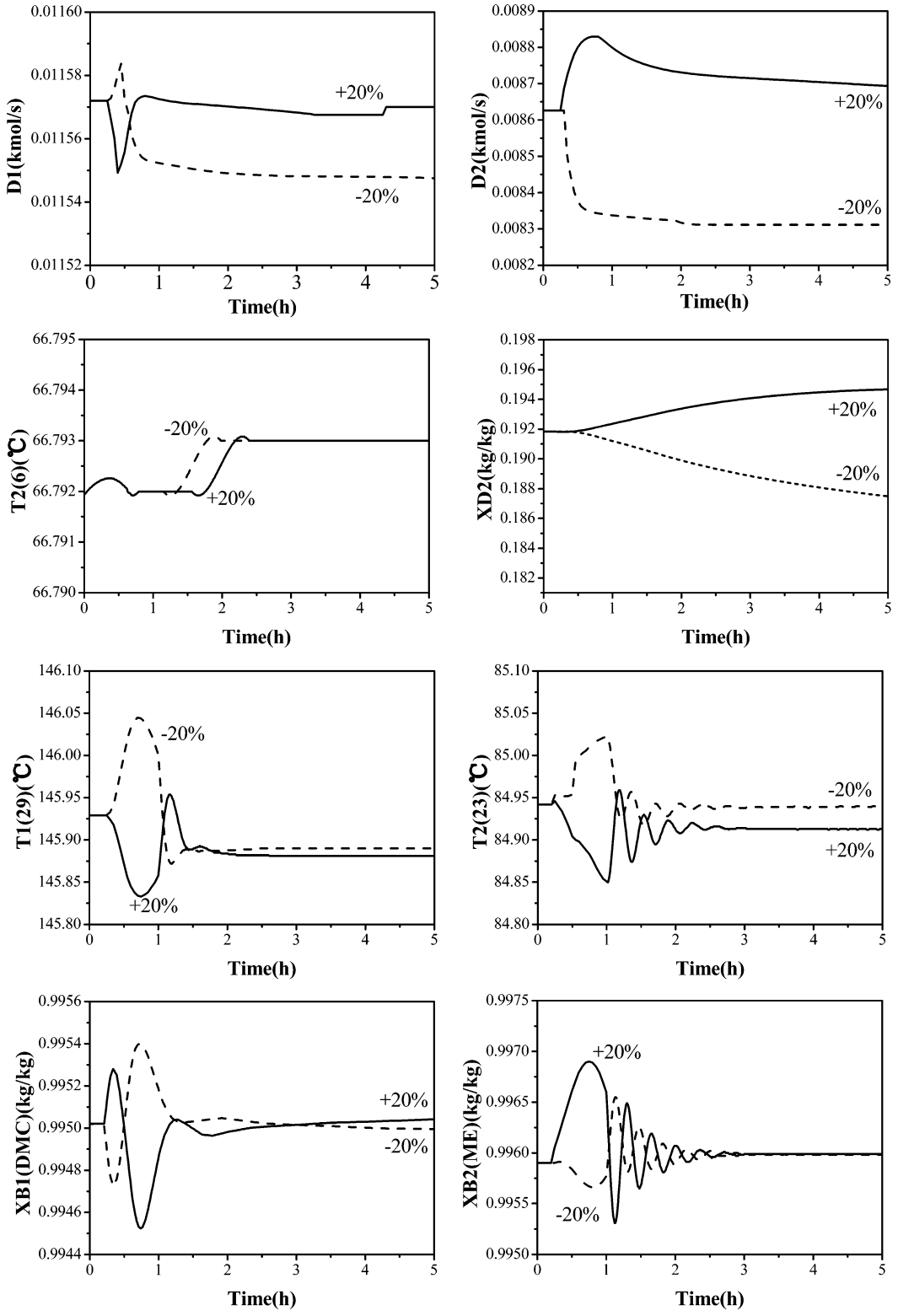

Figure 14. ±20% changes in feed composition.

AUTHOR INFORMATION

Corresponding Author

*E-mail: yhsun@sxicc.ac.cn (Y.H.S.); weiwei@sxicc.ac.cn (W.W.); zhaoning@sxicc.ac.cn (N.Z.).

Notes

The authors declare no competing financial interest.

ACKNOWLEDGMENTS

This work was financially supported by the National Key Technology Research and Development Program of the Ministry of Science and Technology (2013BAC11B00), Ministry of Science and Technology of the People's Republic of China (2009BWZ003), and "Strategic Priority Research Program-Climate Change: Carbon Budget and Related Issues"

of the Chinese Academy of Sciences, Grant No. XDA05010109, XDA05010110, XDA05010204.

NOMENCLATURE

TAC = total annual cost ($/y)
N_T = total number of column trays
N_F = feed tray location of a column
D = distillate flow rate (kmol/s)
B = bottom flow rate (kmol/s)
RR = reflux ratio
D/F = distillate to feed ratio
L = the length of the vessel
D = column diameter (m)
Q_R = reboiler heat input (GJ/h)
Q_C = condenser heat removal (GJ/h)
A_R = reboiler heat transfer areas (m^2)
A_C = condenser heat transfer areas (m^2)
shell = capital cost of the shell (10^6)
HX = heat exchanger cost (10^6)
energy = cost of energy (10^6/y)
R/F = reflux to feed ratio
CC/TC = cascade composition/temperature control structure
CS1 = first control syrtegy
CS2 = second control syrtegy
Q_R/F = the ratio of reboiler heat input to feed
Q_{R1}/F_1 = the ratio of reboiler heat input to feed in the pressurized column
Q_{R2}/F_2 = the ratio of reboiler heat input to feed in atmospheric column
X_{B1} = DMC purity at the bottoms of pressurized column
X_{B2} = ME purity at the bottoms of atmospheric column
$T_{1,29}$ = 29th stage of the pressurized column
$T_{2,6}$ = sixth stage of the atmospheric column
$T_{2,23}$ = 23th stage of the atmospheric column
PI = proportional and integral
K_c = gain
τ_1 = integral time
X_{D1}(ME) = ME product purity in distillate stream of the pressurized column
X_{D2}(DMC) = DMC product purity in distillate stream of the atmospheric column
X_{B1}(DMC) = DMC product purity in bottom stream of the pressurized column
X_{B2}(ME) = ME product purity in bottom stream of the atmospheric column
L_R = reflux flow
V_R = vapor flow rate on the second stage in distillation column
V_S = vapor flow rate from the bottom of the column
L_S = liquid flow rate on the second stage of the column
V_S/F = ratio of the vapor flow rate from the bottom of the column to the feed flow rate

REFERENCES

(1) Delledonne, D.; Rivetti, F.; Romano, U. Developments in The Production and Application of Dimethyl Carbonate. *Appl. Catal. A. Gen.* **2001**, *221* (1−2), 241−251.
(2) Jiang, Z.; Wang, Y. Preparation of Dimethyl Carbonate through Transesterification in a Catalytic Distillation Column. *Chem. Eng.* **2011**, *3*, 29−61.
(3) Delledonne, D.; Rivetti, F.; Romano, U. Developments in the Production and Application of Dimethyl Carbonate. *Appl. Catal., A* **2001**, *221*, 241−251.
(4) Pacheco, M. A.; Marshall, C. L. Review of Dimethyl Carbonate (DMC) Manufacture and Its Characteristics as a Fuel Additive. *Energy Fuels* **1997**, *11* (1), 2−29.
(5) Lü, X.; Yang, G.; Zhang, W.; Zhen, H. Improving the Combustion and Emissions of Direct Injection Compression Ignition Engines Using Oxygenated Fuel Additives Combined with a Cetane Number Improver. *Energy Fuels* **2005**, *19* (5), 1879−1888.
(6) Crandall, J. W.; Deitzler, J. E.; Kapicak, L. A.; Poppelsdorf, F. *Process for the Hydrolysis of Dialkyl Carbonates*. U.S. Patent 4,663,477, May 5, 1987.
(7) Zhang, Q.; Zhong, J.; Wang, Y.; Zhao, M. Study on Extractive Distillation of Dimethyl Carbonate from Its Azeotrope with Methanol Using Toluene as Extracting Agent[J]. *Nat. Gas Chem. Ind.* **2005**, *30* (4), 51−54.
(8) Won, W.; Feng, X.; Lawless, D. Separation of Dimethyl Carbonate/Methanol/Water Mixtures by Pervaporation Using Cross-linked Chitosan Membranes. *Sep Purif Technol.* **2003**, *31* (2), 129−140.
(9) Han, P.; Li, Y.; Wang, Y. Development in Separation of Dimethyl Carbonate-methanol Azeotrope. *J. Jiang Su Polytechn. Univ.* **2003**, *15* (4), 61−63.
(10) Wei, T.; Wang, M.; Wei, W.; Sun, Y.; Zhong, B. Synthesis of Dimethyl Carbonate by Transesterification over CaO/Carbon Composites. *Green Chem.* **2003**, *5* (3), 343−346.
(11) Romano, U.; Tesel, R.; Mauri, M. M.; Rebora, P. Synthesis of Dimethyl Carbonate from Methanol, Carbon Monoxide, and Oxygen Catalyzed by Copper Compounds. *Ind. Eng. Chem. Process. Des. Dev.* **1980**, *19* (3), 396−403.
(12) Itoh, H.; Watanabe, Y.; Mori, K.; Umino, H. Synthesis of Dimethyl Carbonate by Vapor Phase Oxidative Carbonylation of Methanol Presented at the First International Conference on Green & Sustainable Chemistry. *Green Chem.* **2003**, *5* (5), 558−562.
(13) Yamamoto, Y.; Matsuzaki, T.; Tanaka, S.; Nishihira, K.; Ohdan, K.; Nakamura, A.; Okamoto, Y. Catalysis and Characterization of Pd/NaY for Dimethyl Carbonate Synthesis from Methyl nitrite and CO. *J. Chem. Soc., Faraday Trans.* **1997**, *93* (20), 3721−3727.
(14) Jiang, R.; Wang, S.; Zhao, X.; Wang, Y.; Zhang, C. The Effects of Promoters on Catalytic Properties and Deactivation−Regeneration of the Catalyst in the Synthesis of Dimethyl Carbonate. *Appl. Catal. A: Gen.* **2003**, *238* (1), 131−139.
(15) Bayer, A. G. *Process for the Preparation of Carbonic Esters*. European Patent 0,061,677, March 19, 1982.
(16) Saleh, R. Y.; Michaelson, R. C.; Suciu, E. N.; Kuhlmann, B. *Process for Manufacturing Dialkyl Carbonate from Urea and Alcohol*. U.S. Patent 5,565,603, October 15, 1996.
(17) Ryu, J. Y. *Process for Making Dialkyl Carbonates*. U.S. Patent 5,902,894, May 11, 1999.
(18) Sun, J.; Yang, B.; Lin, H. A Semicontious Process for the Synthesis of Methyl Carbamate from Urea and Methanol. *Chem. Eng. Technol.* **2004**, *27* (4), 435−439.
(19) Li, X.; Lian, Y.; Zhang, Z.; Jia, Q.; Liu, L. Separation of Dimethyl Carbonate-Methanol Mixture by Extractive Distillation. *Chem. Eng.* **2012**, *40* (7), 14−17 + 25.
(20) Matsuda, H.; Takahara, H.; Fujino, S.; Constantinescu, D.; Kurihara, K.; Tochigi, K.; Ochi, K.; Gmehling, J. Selection of Entrainers for the Separation of the Binary Azeotropic System Methanol+Dimethyl Carbonate by Extractive Distillation. *Fluid Phase Equilib.* **2011**, *310* (1−2), 166−181.
(21) Wang, L.; Han, X.; Li, J.; Zhan, X.; Chen, J. Separation of Azeotropic Dimethyl Carbonate/Methanol Mixtures by Pervaporation: Sorption and Diffusion Behaviors in the Pure and Nano Silica Filled Pdms Membranes. *Sep. Sci. Technol.* **2011**, *46* (9), 1396−1405.
(22) Zhang, J.; Wang, F.; Peng, W.; Xiao, F.; Wei, W.; Sun, Y. Process Simulation for Separation of Dimethyl Carbonate and Methanol Through Atmospheric-Pressurized Rectification. *Petr. Technol.* **2010**, *39* (6), 646−650.

(23) Fan, W.; Wang, X.; Li, W.; Xiao, W. Adsorption Separation of Dimethyl Carbonate and Methanol Azeotrope. *Chem. Eng.* **2010**, *38* (1), 10−13.
(24) Romano UGO. *Recovery of Dimethyl Carbonate from Its Azeotropic Mixture With Methanol*. German Patent. 2,607,003, Sep 2, 1976.
(25) Katsushige, H.; Koho, K. T. *Separation of Methanol from Dimethyl Carbonate*. Japan Patent 06,228,026 [94228026], (Cl, C07C27ö 34), Aug 16, 1994.a
(26) Luyben, W. L. Comparison of Pressure-Swing and Extractive-Distillation Methods for Methanol-Recovery Systems in the TAME Reactive-Distillation Process. *Ind. Eng. Chem. Res.* **2005**, *44* (15), 5715−5725.
(27) Modla, G.; Lang, P. Removal and Recovery of Organic Solvents From Aqueous Waste Mixtures By Extractive and Pressure Swing Distillation. *Ind. Eng. Chem. Res.* **2012**, *51* (35), 11473−11481.
(28) Luyben, W. L. Design and Control of A Fully Heat-Integrated Pressure-Swing Azeotropic Distillation System. *Ind. Eng. Chem. Res.* **2008**, *47* (8), 2681−2695.
(29) Gilp rin J. A.; Emmons A. H. *Synthesis of DMC*. U.S. patent 3,803,201, April 9, 1977.
(30) Li, C.; Zhang, X.; Zhang, S.; Xu, Q. Vapor-Liquid Equilibria and Process Simulation for Separation of Dimethyl Carbonate and Methanol Azeotropic System. *Chin. J. Process Eng.* **2003**, *3* (5), 453−458.
(31) Wang, S.; Yu, C.; Huang, H. Plant-Wide Design and Control of DMC Synthesis Process via Reactive Distillation and Thermally Coupled Extractive Distillation and Thermally Coupled Extractive Distillation[J]. *Comput. Chem. Eng.* **2010**, *34* (3), 361−373.
(32) Hsu, K. Y.; Hsiao, Y. C.; Chien, I. L. Design and Control of Dimethyl Carbonate-Methanol Separation via Extractive Distillation in The Dimethyl Carbonate Reactive Distillation Process. *Ind. Eng. Chem. Res.* **2010**, *49* (2), 735−749.
(33) Repke, J. U.; Forner, F.; Klein, A. Separation of Homogeneous Azeotropic Mixtures by Pressure Swing Distillation-Analysis of the Operation Performance. *Chem. Eng. Technol.* **2005**, *28* (10), 1151−1157.
(34) Varbanov, P.; Klein, A.; Repke, J. U.; Wozny, G. Minimising the Startup Duration for Mass- and Heat-Integrated Two-Column Distillation Systems: A Conceptual Approach. *Chem. Eng. Prog.* **2008**, *47*, 1456.
(35) Repke, J. U.; Klein, A.; Bogle, D.; Wozny, G. Pressure Swing Batch Distillation for Homogeneous Azeotropic Separation. *Chem. Eng. Res. Des.* **2007**, *85* (A4), 492.
(36) Löwe, K.; Wozny, G. A New Strategy for Product Switchover and Startup for A Heat- and Mass-Integrated Distillation System. *Chem. Eng. Process* **2001**, *40*, 295.
(37) Modla, G.; Lang, P. Feasibility of New Pressure Swing Batch Distillation Methods. *Chem. Eng. Sci.* **2008**, *63* (11), 2856−2874.
(38) Luyben, W. L. Pressure-Swing Distillation for Minimum- and Maximum-Boiling Homogeneous Azeotropes. *Ind. Eng. Chem. Res.* **2012**, *51* (33), 10881−10886.
(39) Koga, K. *Separation of Dimethyl Carbonate [P]*. Japan patent 2212456, Aug 23, 1990.
(40) Ma, X.; Liu, X.; Li, Z.; Xu, G. Vapor−Liquid Equilibria for The Ternary System Methanol + Dimethyl Carbonate + Dimethyl Oxalate and Constituent Binary Systems at Different Temperatures. *Fluid Phase Equilib.* **2004**, *221* (1−2), 51−56.
(41) Shi, Y.; Liu, H.; Wang, K.; Xiao, W.; Hu, Y. Measurements of Isothermal Vapor−Liquid Equilibrium of Binary Methanol/Dimethyl Carbonate System Under Pressure. *Fluid Phase Equilib.* **2005**, *234* (1−2), 1−10.
(42) Luyben, W. L. *Distillation Design and Control Using Aspen Simulation*; John Wiley &Sons, Inc: New York, 2006.
(43) Luyben, W. L. *Plantwide Dynamic Simulation in Chemical Processing and Control*; Marcel Dekker: New York, 2002.
(44) Grassi, V. G. *Practical Distillation Control*; Van Nostand Reinhold Press: New York, 1992.
(45) Luyben, W. L. Tuning Proportional−Integral−Derivative Controllers for Integrator/Deadtime Processes. *Ind. Eng. Chem. Res.* **1996**, *35* (10), 3480−3483.
(46) Yu, B.; Wang, Q.; Xu, C. Design and Control of Distillation System for Methylal/Methanol Separation. Part 2: Pressure Swing Distillation with Full Heat Integration. *Ind. Eng. Chem. Res.* **2012**, *51*, 1293−1310.
(47) Luyben, W. L. Control of the Maximum-Boiling Acetone/Chloroform Azeotropic Distillation System. *Ind. Eng. Chem. Res.* **2008**, *47* (16), 6140−6149.